Published in final edited form as:
Carbon N Y. 2014 June ; 72: 215–223. doi:10.1016/j.carbon.2014.02.005.

Explosive thermal reduction of graphene oxide-based materials: mechanism and safety implications

Yang Qiu, **Fei Guo**, **Robert Hurt**, and **Indrek Külaots***
School of Engineering, Brown University, 182 Hope St., Providence, RI, USA, 02912

Abstract

Thermal reduction of graphene oxide or graphite oxide (GO) is an important processing step in the fabrication of many graphene-based materials and devices. Here we show that some bulk solid GO samples can undergo explosive decomposition when small samples are heated slowly in inert gas environments, while others do not. These micro-explosions can occur for samples as small as few milligrams and are sufficiently energetic to cause laboratory equipment damage. Thermochemical analysis methods are used to understand the factors that lead to the explosive reduction mode. The studies show that the explosive mode of reduction is caused by the exothermicity of GO reduction coupled with a threshold sample mass/size that causes heat and mass transfer limitations leading to local temperature rise and a thermal runaway reaction. The explosive mode of reduction is not caused or promoted by interstitial water, and its onset temperature can be lowered by immersion in potassium hydroxide solution. By allowing early release of internal gas pressure, the explosive mode reduces the extent of surface area development in GO exfoliation from an optimum value of 1470 m^2g^{-1} obtained under non-explosive reduction conditions. Explosive reduction of bulk GO poses industrial safety hazards during large-scale storage, handling, and processing.

1. Introduction

Graphene oxide and graphite oxide (GO) are promising precursors for large-scale manufacture of graphene-based carbon materials. GO can be thermally or chemically treated to obtain reduced graphene oxide (rGO), which partially restores the electrical conductivity and hydrophobicity of pristine graphite for use as a 2D composite filler or conducting film. Monolayer GO processing can lead to massive area loss (for example from 2600 to 40 m^2g^{-1} [1]) due to alignment and face-to-face stacking during GO deposition and drying [1]. Thermal exfoliation of bulk GO (graphite oxide) is attractive for large-scale production of GO-derived few-layer-graphene flakes [2], or expanded graphene-based powders with high porosity and surface area for catalysis, separation, or gas storage applications. The heating of GO in inert gas is commonly called “thermal reduction” in the field because the main goal is to produce the reduced, graphene-like solid product, rGO. Strictly speaking, it is not a reduction since there is no external reducing agent, but is rather a chemical disproportionation, in which the original carbon atoms partition into reduced forms in solid rGO and oxidized forms that are primarily carbon oxide gas-phase byproducts (CO, CO_2). Thermal reduction of multilayer GO has been extensively investigated [3–9]. High vacuum

*Corresponding author. Tel: 401 863-2674. Indrek_Kulaots@brown.edu (Indrek Külaots).

has been reported to support low temperature exfoliation (below about 300°C) by increasing the mechanical driving force for flake expansion, which is the difference between the internal (interstitial) pressure and the environmental pressure [6, 9]. Porous materials from photothermal reduction of graphene oxide papers have been prepared by Mukherjee et al. [10] for lithium-ion battery applications. The presence of H_2 in the surrounding gas phase and pretreatment of GO with HCl have both been shown to enhance the thermal exfoliation of graphite oxide [11]. Higher rates of thermal exfoliation are obtained by rapid release of the highly volatile HCl, which creates additional overpressure needed to successfully overcome van der Waals forces between GO sheets. In addition, hydrogen in gas environment during reduction can violently react to –OH functionality in GO, and induce thermal decomposition [11]. Thermal exfoliation in GO induces the decomposition of epoxides and hydroxyls, the rate of which competes with the diffusion rate of the reaction products CO_2 and CO decomposition. Successful thermal exfoliation is achieved when rate of decomposition of GO exceeds the rate of diffusion of gas products and needed threshold overpressure is built between individual GO layers [12]. Increasing O/C ratio of GO [4] increases GO decomposition rate and therefore, will enhance thermal exfoliation due the build up of larger gas volumes during reduction. For the successful thermal exfoliation overpressure is needed to overcome the van der Waals forces existing between the two adjacent GO layers [12].

It is well known that GO can be thermally unstable and should be regarded as an energetic material [13–15]. Nanoscale GO made from the oxidative unzipping of carbon nanotubes can also undergo explosive decomposition if heated in N_2 gas [16]. Kim et al. [14] and Krishnan et al. [15] report the spontaneous ignition of GO films in air under the influence of potassium residues that act as a catalyst for the carbon combustion reaction: $C + O_2 \Rightarrow CO/CO_2$, where “C” represents the rGO film. GO thermal reduction or disproportionation reaction is typically conducted in the absence of air, either in vacuum or inert gas blanket to protect the rGO product. Under these inert conditions there have been observations of a “popping” behavior - rapid GO reduction with sudden onset in some experiments [2, 12], but no systematic studies of the factors that determine whether a given sample will exhibit the explosive or non-explosive mode.

We hypothesized that the self-initiating rapid reduction of GO with large-volume gas release would show features in common with other energetic materials (explosives and mono-propellants) [17–19] and of some reactive chemicals that represent important safety concerns in industry [20–22], and must be understood and characterized for the safe handling of GO, especially at large scale. In the present study, we observe explosive decomposition during the thermal reduction of GO in inert gas environments leading to laboratory equipment damage, which occurs for some GO samples, but not others. We systematically explore the thermochemistry and mechanism of this energetic behavior and discuss its implications for safe GO processing and scale-up.

2. Experimental section

GO was prepared by a modified Hummers method [23] including the pre-oxidation treatment. The sample was further purified by a two-step acid-acetone wash to remove the

salt byproducts [14]. The raw GO product was stored in the form of a lump, bulk solid, or GO cake (graphite oxide). The current experiments use solid samples from this GO cake directly, and in other experiments use multilayer films formed by depositing sets of GO monolayers from aqueous suspensions derived from the same cake.

The GO multilayer films were prepared by pipetting 2 $mgml^{-1}$ GO solution onto clean polystyrene substrate and left to dry at room temperature overnight (see procedure schematic in supporting information section of manuscript Fig.S1a). Each day the thickness of the existing GO film was increased by pipetting fresh 2 $mgml^{-1}$ GO solution on top of the previously dried film until the desired cycle number (cycle corresponds to each day) GO drop-cast film thickness was achieved. After drying was complete the x-cycle number GO film was peeled off from the polystyrene surface [see GO films in Figures S1b and S1c]. The total number of graphene oxide layers in each film can estimated from:

$$N=(m/A)/\rho\delta \quad (1)$$

where ρ is the material density, δ the interlayer spacing, *m* mass of GO and *A* the area of GO sample used.

Drop-cast GO film and GO cake reduction experiments were performed in a differential scanning calorimeter (DSC) model 2910 from TA Instruments and thermogravimetric apparatus model 951 from TA Instruments in nitrogen gas flow. The heating rates applied were 10 to 50 $Kmin^{-1}$ and the maximum thermal reduction temperature 250°C. The surface morphology and the chemical composition of the rGO samples were characterized by field emission SEM with energy dispersive X-ray analysis (SEM-EDX). The metals content of GO cake samples was characterized by inductively coupled plasma emission spectroscopy (ICP-ES). The 77K N_2 and 273K CO_2 adsorption isotherms were recorded applying Autosorb-1 instrument from Quantachrome, Inc. The BET surface areas were calculated from N_2 adsorption isotherms using relative pressures ranging from 0.05 to 0.30, if nearly perfect linear BET correlations were observed. All surface area values were recorded when linear BET correlation factor was at least $R^2 = 0.9999$. Pore size distributions (PSD) were calculated applying non-local density functional theory (NLDFT) slit pore model [24, 25].

3. Results and Discussion

3.1 Thermochemistry and rates of GO reduction

During the course of GO thermal reduction experiments in the laboratory, we sometimes observed violent decomposition events in the TGA during $10Kmin^{-1}$ heating in inert gas that resulted in loss of sample from the pan, failure of the experiment, and coating of very fine powder product throughout the interior of the device. The event was reproducible. More dramatically we observed an explosive decomposition in the DSC leading to interruption and failure of the experiment as well as DSC cell damage as shown in Fig.S2b. The metal DSC hermetic sample pan was torn into two parts, the reference pan was displaced and graphene-derived powder was spread throughout the cell (Fig.S2b). Images from the TGA experiment are also presented in Fig.S2c (before micro-explosion) and in Fig.S2d (after micro-explosion). In other reduction experiments in TGA and DSC, the integrity of the solid

GO body was preserved. We hypothesized this damage was the result of a thermal runaway reaction driven by the exothermicity of GO reduction. We had not appreciated the potential for equipment damage when processing small amounts of GO, and were intrigued that some samples behaved energetically in inert gas, while others did not.

We therefore investigated the thermochemistry of GO reduction by employing uniform multilayer films of controlled thickness in DSC (see example thermogram shown in Fig.1a) and in TGA (see example TGA curves on Fig.1b and Fig.1c.). Thermal reduction of 15-cycle drop-cast film leads to a large exothermic peak in DSC, with decomposition ΔH of approximately 1,680 Jg^{-1}. The onset temperature for the exothermic transition occured near 150°C. This decomposition enthalpy (1,680 Jg^{-1}) corresponds to an estimated adiabatic final temperature of 1,240°C, calculated for the case where the onset temperature is 150°C and the product distribution is 40 wt-% gas (CO_2) and 60 wt-% carbonaceous (graphite) product. Adiabatic flame temperature was estimated from:

$$\Delta H = \int_{T_o}^{T_a} C_p dT \quad (2)$$

where T_a is adiabatic temperature, T_o onset temperature, ΔH – enthalpy change related to decomposition (obtained experimentally), C_p sum of specific heat capacities of CO_2 (polynomial applied) and of pure graphite.

In the experiment of Fig.1a, the heat evolution was continuous and smooth and the decomposition reaction in this GO film form did not produce a violent micro-explosion or sensitive equipment damage. We hypothesize that the thin film structure allows sufficiently fast heat transfer to prevent local temperature rise and thermal runaway, and allows sufficiently fast mass transfer of gas phase products to prevent internal pressure build-up and rGO film disintegration. Similar behaviour is seen when the 15-cycle drop-cast GO film was tested in TGA in inert gas environment. The GO film reduction does produce a porous rGO product, but does not explode (see rGO films on SEM images in Fig.1d and Fig.1e). The total mass loss in our GO decomposition is approxiamely 40 wt-% (not including water, see TGA example curve in Fig.1b), suggesting that our GO film has relatively high O/C ratio (30 wt-% reported in [2, 12]). Table 1 summarizes the DSC results for a number of experiments using GO samples of different form (cake or film) and mass. The temperatures at the peak of the DSC exotherm reported in Table 1 for all GO films are within the reported decomposition range for oxygen-containing functional groups on GO. As the drop-cast GO film thickness increases (while keeping the lateral area the same), the total energy released during GO decomposition increases linearly, and the correlation is independent of heating rates tested 10 or 50 $Kmin^{-1}$. The specific exothermic GO decomposition heat released is quite significant and is reproducible in the range 1400 to 1650 Joules per gram of GO, which is similar to the 1500 Jg^{-1} reported in [12]. Krishnan et al. [15] reports a significantly higher exothermic decomposition enthalpy of 6 – 8 kJg^{-1}, which may be due to differences in synthesis or to aging effects [26], which require more study. All thermochemical data in Table 1 originate from the same original GO synthesis batch and none of these uniform multilayer films underwent explosive decomposition in this set of experiments, so the calorimetry results are quantitatively reliable. The FTIR scan results of 15-cycle drop-cast GO film and the same rGO film are shown on Figure S3c. As seen GO film investigated has

wide hydroxyl peak (ranging between 2900–3600 cm^{-1}), together with epoxides (962 cm^{-1}), ethers (1035 cm^{-1}) and carboxyls (1724 cm^{-1}). The 1619 cm^{-1} peak is related to vibrations from the unfunctionalized graphenic domains of GO. During thermal exfoliation in inert gas most of the oxides are removed when heated to 250°C. This result is consistent what has been as seen by others [2, 12]. Our SEM-EDX results give an average C/O atomic ratio of ~1.8 in our GO samples.

3.2 Morphology and pore structure of the rGO products

The surface area and porosity of the rGO samples listed in Table 1 were investigated both with N_2 and CO_2 probes. The N_2 and CO_2 adsorption analysis for BET surface area and PSD revealed that GO films prior to reduction have very low surface area, similar to those reported [1, 6, 27]. For example, 3 and 6 cycle drop-cast GO film N_2 BET surface areas are 0.25 and 0.21 m^2g^{-1}, respectively and the corresponding thermally reduced samples have only slightly higher surface area of 0.85 m^2g^{-1}. Therefore, low-temperature, low-heating-rate, atmospheric-pressure thermal reduction of thin GO films leads to relatively non-porous rGO. When a thicker film (15-cycle drop-cast) is reduced in DSC (SEM image shown on Fig. 1e) we obtain much higher area values: an N_2 surface area of 171 m^2g^{-1}, and a CO_2 BET area as large as 1471 m^2g^{-1}. To our knowledge this is the largest surface area reported for thermally reduced GO films. As the pore size distribution shows (Fig.1f) most of this vast surface area originates from super-micropores – those with pore sizes approximately 0.35 nm. This is the micro-pore size range that can show molecular sieving behavior and allows access to CO_2 at 273 K, but not to N_2 at 77 K due to activated diffusion processes [28].

Returning to the forensic investigation of why certain GO samples explode during thermal reduction, we examined the rGO powder product obtained after the micro-explosions of the GO cake in the DSC. Powders from the GO cake reduction were carefully removed from DSC cell (Fig.S2b) and from the TGA pan (Fig.S2d), and imaged in SEM (Fig.2a,b). In Fig. 2a the individual rGO particles are seen to have a highly irregular shape and with a lateral dimension from 1 to 3 μm. The SEM image on Fig.2b reveals that the powder shown in Fig. 2a is multi-layer rGO platelet. Fig. 2c and 2d show the N_2 adsorption isotherm of the same rGO powder obtained after GO cake micro-explosion together with the pore size distribution (PSD) applying the non-local density function theory (NLDFT) slit pore model [24, 25]. The BET N_2 surface area of the GO cake is only 2 m^2g^{-1}, while the exploded rGO cake product N_2 BET surface area is 300 m^2g^{-1}, implying a mean apparent layer number per stack of 8–9 using the scaling law $S.A \sim 2600N^{-1}$ [1]. The CO_2 BET surface area of GO cake is in the same magnitude as sensed with N_2, but somewhat larger at 502 m^2g^{-1}, likely due to accessible internal super-microporosity. Interestingly, the rGO powder surface area is approximately 3 orders of magnitude smaller than the CO_2 BET surface area of non-exploded 15-cycle drop-cast rGO film as reported above 1471 m^2g^{-1}. This is an interesting finding, as it suggests that the micro-explosion is not necessarily desirable for achieving the highest possible surface area. The lower surface area in the exploded sample may be due to early release of the internal pressure when the film undergoes multipoint mechanical fracture partway through the gas evolution process. Samples that evolve gas quickly but not

fast enough to explosively fracture likely develop the highest internal pressures to overcome interlayer van der Waals forces.

The PSD of GO cake powder (Fig.2d insert) reveals an interesting periodicity, which is similar to pore size periodicity reported in [1]. This type of periodicity can be evidenced when investigating porosity of solid few-layer GO (FLGO) when each particle is considered as thick platelet, which stay mostly non-porous and have relatively uniform thickness. The primary porosity generated in this type of GO system originates from the external surfaces of the multilayer rGO plates. A close examination of the PSD presented on Fig.2d insert suggests that the rGO plate thickness can be approximated to be 4 nm. Therefore suggesting that each rGO plate would include approximately 11 individual rGO sheet layers. From this layer number BET area is calculated to be 250 m^2g^{-1} (applying power-law, $S.A = 2600N^{-1}$ as shown in [1]). This area result is in reasonable agreement with the measured 300 m^2g^{-1} N_2 BET surface area.

3.3 Role of water, potassium hydroxide, and sample mass in explosive reduction

A series of control experiments were made to understand the mechanism of explosive reduction and the dependence on GO sample properties. Figure 3a shows a DSC thermogram of GO thermal reduction for an 8 mg cake sample in a sealed aluminum hermetic pan in inert gas. This is one of the GO cake experiments that produced explosive decomposition (see image in Fig.S2b for micro-explosion photo evidence). The DSC thermogram on Fig.3a shows a very clear endothermic water peak with the maximum occurring at 126°C. The water removed at this temperature is likely bound water trapped between individual GO sheets by hydrogen bonding. The free external water is removed at around 50°C (see differential TGA curve Fig.1c), which DSC thermogram on Fig.3a does not show. As seen in thermogram Fig.3a the smooth endothermic water peak is followed by a GO thermal reduction exotherm, and in this case the peak is asymmetric and truncated with a smooth rise on the low-temperature side and an abrupt cliff on the high-temperature side. Throughout our DSC experiments, this type of truncated exotherm peak correlates with the presence of the explosive event. The GO micro-explosion is preceded by a slight inflection in the DSC curve caused by local temperature rise (see arrow Fig. 3a) that signals the runaway reaction, followed by a peak and abrupt decay as the sample pan loses contact with the DSC sensor. The onset temperature of the GO runaway reaction in this experiment is about ~155°C and the peak temperature is ~171°C. We initially thought that interstitial water might be responsible for the violent GO micro-explosion during reduction in DSC by providing additional gas volume to increase internal interstitial pressure.

In order to test the hypothesis that water is responsible of these micro-explosions, we oven-dried the GO cake sample that was known to explode (DSC thermogram shown on Fig.3a) overnight at relative low temperatures (~80°C) and repeated the DSC experiment in inert gas environment with heating rate 10 $Kmin^{-1}$. Fig.3b shows the oven-dried GO cake thermogram, which now is missing the endothermic water peak, but still ended with micro-explosion. Since the water endothermic peak is missing, one can easily determine the onset temperature of the GO thermal reduction as 140°C. In order to further investigate the possible role of water in GO explosive reduction we humidified one of the GO cake samples

that was known not to explode in a fully saturated water vapor environment at ambient temperature overnight. The thermogram in Fig.3c shows a very large endotherm, but the experiment did not end with the micro-explosion. One can note the large water endothermic peak, which specific heat determined from thermogram and the mass of water removed closely matches with the latent heat of water of evaporation 2,200 Jg^{-1} at ambient pressure. The thermal reduction onset temperature is now at approximately 160°C, which is approximately ~20°C higher temperature if compared to GO cake onset temperature provided on Fig.3b. Note the smoothness of exothermic GO thermal reduction peak. The heat and mass generated during reduction has time to dissipate, and therefore the sample did not explode. These control experiments clearly show that water is not necessary for the explosive reduction of GO and does not promote the explosive mode of reduction. GO explosive decomposition is occurring in the dry state.

Further control experiments were conducted to see if explosive reduction is related to impurities. GO synthesis involves potassium permanganate $KMnO_4$ and samples may contain residual potassium [14, 15]. Potassium has been reported to cause GO ignition through catalysis of the combustion reaction [14, 15], but there is no air in the current experiments, so combustion catalysis is not a possible mechanism. As a control experiment we used a GO cake sample that did not explode in the DSC (see smooth thermogram in Fig. 4a) and immersed it into 1 wt-% KOH solution and repeated the DSC experiment (10 $Kmin^{-1}$ in N_2 gas). The resulting DSC thermogram is shown in Fig.4b. There is no water endotherm present, and the cake did explode, indicating a promoting effect of potassium or hydroxide. In addition, the exotherm onset temperature is about 50°C lower than the undoped GO cake sample (see Fig.4a,b), which is somewhat larger KOH treatment effect than 20°C lower onset temperature observed elsewhere [15]. We conducted SEM EDX and ICP-ES experiments on two of the as-produced samples, only one of which was observed to undergo explosive reduction. The energetic sample had an 8-fold higher potassium (K) content (0.08 atom-%) than the non-energetic sample (0.01 atom-%) by EDX. A more accurate ICP-ES analysis showed K content of 0.0436±0.0017 wt.-% for the energetic sample and 0.0013±0.0003 wt.-% for the non-energetic sample. Together these results suggest that K may play a role in promoting the explosive decomposition of GO. In addition to K's well-known behavior as a catalyst for carbon combustion, $C + O_2 \Rightarrow CO/CO_2$ [14], it has also been reported be catalysts for the pyrolysis of biomass and other oxygenated organic compounds [29–32]. Addition of K to cellulosic material has been reported to increase gas and char (solid) yields, while reducing the yield of higher molecular weight volatiles (tars) [29, 31, 32]. Potassium has been reported to increase CO and CO_2 yield [30] or rate of evolution [29] and to reduce the pyrolysis activation energy by 50 $kJmol^{-1}$ and lower the main pyrolysis temperature by 41–67°C [29], which is very similar to the difference in onset temperatures seen in our GO thermal experiments (see Fig. 4a and 4b). The molecular mechanism of K-catalysis of pyrolysis is not fully understood, but has been proposed to involve K-promoted heterolytic ring opening and cracking reactions [29] and deoxygenation reactions [30]. Alternatively, the catalytic effect of KOH immersion may be due to hydroxide, which can establish basic conditions in the interstitial water phase. Several studies have reported base-catalyzed GO deoxygenation [33–35], which may reduce the

exotherm onset temperatures observed here. More work is needed to understand the effect of impurities and additives on the potential for GO explosive decomposition.

Potassium hydroxide addition promotes GO explosive decomposition and lowers the onset temperature, but it remains to be seen if it is *necessary* for GO explosive decomposition. We therefore conducted series of TGA experiments with varying the GO cake mass. Figure 4c shows TGA thermogram of a GO cake sample known to explode in the DSC under identical heating conditions. The sample undergoes abrupt total mass loss indicating explosive reduction at 162°C, which is similar to the 167°C explosion temperature seen in the DSC. A low-K GO cake that did not explode in DSC was also studied in TGA (see Fig. 4d). As seen this sample does explode, but at 196°C, which is 34°C higher temperature value than the explosion temperature value recorded with high-K GO cake (Fig.4c). Therefore, GO KOH immersion or high K content is not required for explosive GO decomposition.

Figure 4e shows that the explosive reduction of GO can be initiated by simply increasing GO cake mass. In other known energetic materials, thermal runaway reactions occur when decomposition reaction heat cannot be dissipated fast enough to the surroundings, and local temperatures within the sample rise. Decomposition reactions have significant activation energies, and the elevated local temperatures thus cause accelerated decomposition rates and further heating in uncontrolled fashion leading to rapid gas release and pressure waves associated with deflagration or detonation mechanisms [17]. The stability of energetic materials is typically mass dependent, as the rate of heat generation is proportional to L^3 (for 3D bodies), while heat loss is related to surface area (~L^2) and size dependent heat transfer coefficients. For bulk GO samples, large sample mass favors internal buildup of both heat and gaseous reduction products, leading to thermal runaway and explosive exfoliation. It is significant that the explosive reduction can occur for GO sample masses as small as few milligrams.

3.4 Safety implications

Even slow heating of few milligram-sized graphene oxide samples in inert gas can lead to uncontrolled micro-explosions that show the characteristics of thermal runaway reactions. The thermal runaway reaction is caused by the exothermicity of GO decomposition (~ 1600 Jg^{-1}) coupled with heat and mass transfer limitations that become more severe with increasing sample mass. Table 2 shows that GO mass-specific enthalpy of decomposition associated with its thermal reduction is comparable with the decomposition enthalpies of known explosives or monopropellants such as hydrazine [17], trinitrotoluene (TNT) [18], nitrocellulose [19] and hazardous industrial chemicals such as cumene hydroperoxide [21], benzoyl peroxide [22]. The micro-explosions observed here occur for sample masses as low as few milligrams and can damage laboratory equipment, but a potentially more significant concern is the large-scale storage, handling, and processing of bulk graphene oxide as GO-based technologies are piloted and commercialized. The hazards associated with large bulk GO samples include heat generation, fire, gas release and overpressure in vessels, and potential pressure or shock waves when GO undergoes explosive reduction in confined environments or in open air, especially when self heating and self-initiation causes the thermal runaway reaction to occur in an unanticipated way during storage and handling.

Figure 5 shows the results of calculations of heat release, volumetric gas release, and overpressure for a range of conditions and GO sample mass. The common x-axis is the mass of dry bulk GO, and y-axis STP gas volume generated, total energy released (J) due to GO decomposition and overpressure (atm) created if sealed into closed containers with fixed volume (varying container volumes from 1 ml to 100 liters shown curves on Fig.5 top). For example, if 1 gram of GO is used with the mass loss of roughly 40 wt-%, it will generate about 0.20 liters of gas and 1500 Joules of heat. Applying the ideal gas law and a chamber volume 1 ml 150°C temperature (typical GO runaway decomposition temperature), one can calculate the overpressure created during thermal reduction of 1 gram of GO to be 320 atmospheres. The mechanical stresses associated with overpressure may be augmented by pressure waves associated with deflagration or detonation processes. More work on the detailed kinetics and transport processes that govern GO explosive decomposition to understand the behavior as an energetic material.

4. Conclusions

The thermal reduction of graphene oxide samples in inert environments under slow heating can occur in either a controlled, continuous mode, or in an uncontrolled explosive mode. The explosive mode is a thermal runaway reaction driven by the exothermicity of GO reduction coupled with a threshold sample mass or minimum-dimension that retards heat and mass transfer allowing local temperature rise and internal pressure development. Understanding and managing the explosive mode of GO reduction is important for exfoliation efficiency, surface area development, and processing safety. Thermal reduction in the controlled (non-explosive) mode achieves an optimal CO_2 BET surface area as high as 1471 m^2g^{-1}, which originates from pores approximately 0.35 nm in size. Explosive reduction leads to lower surface areas, as fracture causes early gas release that limits internal pressure development. The explosive mode of GO reduction in inert gas is not caused or promoted by the presence of interstitial water. Potassium hydroxide immersion lowers the onset temperature for the GO reduction exotherm and increases the probability of the explosive mode. The intrinsic exothermicity of GO reduction (~1600 Jg^{-1}) is comparable to some hazardous industrial chemicals and explosives, and GO should thus be regarded as an energetic material that represents safety hazards during large-scale storage, handling, and processing. More work is needed to understand the kinetics and mechanisms of the explosive reduction process in order to fully characterize the hazards associated with large-scale GO processing and allow its safe development and commercialization.

Supplementary Material

Refer to Web version on PubMed Central for supplementary material.

Acknowledgments

The authors acknowledge financial support from the Brown-Yale Center for Chemical Innovation (NSF Award CHE-1240020), and the Superfund Research Program of the National Institute of Environmental Health Sciences (Grant P42 ES013660).

References

1. Guo F, Creighton M, Chen Y, Hurt R, Külaots I. Porous structures in stacked, crumpled and pillared graphene-based 3D materials. Carbon. 2014; 66(0):476–484.
2. Zhang C, Lv W, Xie X, Tang D, Liu C, Yang Q-H. Towards low temperature thermal exfoliation of graphite oxide for graphene production. Carbon. 2013; 62(0):11–24.
3. Du QL, Zheng MB, Zhang LF, Wang YW, Chen JH, Xue LP, et al. Preparation of functionalized graphene sheets by a low-temperature thermal exfoliation approach and their electrochemical supercapacitive behaviors. Electrochim Acta. 2010; 55(12):3897–3903.
4. Jin M, Jeong HK, Kim TH, So KP, Cui Y, Yu WJ, et al. Synthesis and systematic characterization of functionalized graphene sheets generated by thermal exfoliation at low temperature. J Phys D Appl Phys. 2010; 43(27)
5. Jung I, Dikin DA, Piner RD, Ruoff RS. Tunable electrical conductivity of individual graphene oxide sheets reduced at "low" temperatures. Nano Lett. 2008; 8(12):4283–4287. [PubMed: 19367929]
6. Lv W, Tang DM, He YB, You CH, Shi ZQ, Chen XC, et al. Low-temperature exfoliated graphenes: vacuum-promoted exfoliation and electrochemical energy storage. Acs Nano. 2009; 3(11):3730–3736. [PubMed: 19824654]
7. Schniepp HC, Li JL, McAllister MJ, Sai H, Herrera-Alonso M, Adamson DH, et al. Functionalized single graphene sheets derived from splitting graphite oxide. J Phys Chem B. 2006; 110(17):8535–8539. [PubMed: 16640401]
8. Ye J, Zhang HY, Chen YM, Cheng ZD, Hu L, Ran QY. Supercapacitors based on low-temperature partially exfoliated and reduced graphite oxide. J Power Sources. 2012; 212:105–110.
9. Zhang HB, Wang JW, Yan Q, Zheng WG, Chen C, Yu ZZ. Vacuum-assisted synthesis of graphene from thermal exfoliation and reduction of graphite oxide. J Mater Chem. 2011; 21(14):5392–5397.
10. Mukherjee R, Thomas AV, Krishnamurthy A, Koratkar N. Photothermally reduced graphene as high-power anodes for lithium-ion batteries. Acs Nano. 2012; 6(9):7867–7878. [PubMed: 22881216]
11. Shen B, Lu DD, Zhai WT, Zheng WG. Synthesis of graphene by low-temperature exfoliation and reduction of graphite oxide under ambient atmosphere. J Mater Chem C. 2013; 1(1):50–53.
12. McAllister MJ, Li JL, Adamson DH, Schniepp HC, Abdala AA, Liu J, et al. Single sheet functionalized graphene by oxidation and thermal expansion of graphite. Chem Mater. 2007; 19(18):4396–4404.
13. Jimenez PSV. Thermal-decomposition of graphite oxidation-products DSC studies of internal-combustion of graphite oxide. Mater Res Bull. 1987; 22(5):601–608.
14. Kim F, Luo JY, Cruz-Silva R, Cote LJ, Sohn K, Huang JX. Self-propagating domino-like reactions in oxidized graphite. Adv Funct Mater. 2010; 20(17):2867–2873.
15. Krishnan D, Kim F, Luo JY, Cruz-Silva R, Cote LJ, Jang HD, et al. Energetic graphene oxide: challenges and opportunities. Nano Today. 2012; 7(2):137–152.
16. Cataldo F, Compagnini G, D'Urso L, Palleschi G, Valentini F, Angelini G, et al. Characterization of graphene nanoribbons from the unzipping of MWCNTs. Fuller Nanotub Car N. 2010; 18(3): 261–272.
17. Jang IJ, Shin HS, Shin NR, Kim SH, Kim SK, Yu MJ, et al. Macroporous-mesoporous alumina supported iridium catalyst for hydrazine decomposition. Catal Today. 2012; 185(1):198–204.
18. Ksiazczak A, Ksiazczak T. Influence of DSC measurement conditions on kinetic parameters of thermal decomposition of 2,4,6-trinitrotoluene. J Therm Anal Calorim. 2000; 60(1):25–33.
19. Sovizi MR, Hajimirsadeghi SS, Naderizadeh B. Effect of particle size on thermal decomposition of nitrocellulose. J Hazard Mater. 2009; 168(2–3):1134–1139. [PubMed: 19398264]
20. Cataldo F. Chemical and thermochemical aspects of the ozonolysis of ethyl oleate: decomposition enthalpy of ethyl oleate ozonide. Chem Phys Lipids. 2013; 175:41–49. [PubMed: 23969233]
21. Di Somma I, Andreozzi R, Canterino M, Caprio V, Sanchirico R. Thermal decomposition of cumene hydroperoxide: chemical and kinetic characterization. Aiche J. 2008; 54(6):1579–1584.
22. Severini F, Gallo R. Differential scanning calorimetry ctudy of thermal-decomposition of benzoyl peroxide and 2,2'-azobisisobutyronitrile mixtures. J Therm Anal. 1984; 29(3):561–566.

23. Hummers WS, Offeman RE. Preparation of graphitic oxide. Journal of the American Chemical Society. 1958; 80(6) 1339-.
24. Lastoskie C, Gubbins KE, Quirke N. Pore-size heterogeneity and the carbon slit pore - a Density-Functional Theory model. Langmuir. 1993; 9(10):2693–2702.
25. Ravikovitch PI, Vishnyakov A, Russo R, Neimark AV. Unified approach to pore size characterization of microporous carbonaceous materials from N-2, Ar, and CO2 adsorption isotherms. Langmuir. 2000; 16(5):2311–2320.
26. Kim S, Zhou S, Hu YK, Acik M, Chabal YJ, Berger C, et al. Room-temperature metastability of multilayer graphene oxide films. Nat Mater. 2012; 11(6):544–549. [PubMed: 22561900]
27. Yang SJ, Kim T, Jung H, Park CR. The effect of heating rate on porosity production during the low temperature reduction of graphite oxide. Carbon. 2013; 53:73–80.
28. Lozano-Castello D, Cazorla-Amoros D, Linares-Solano A. Usefulness of CO2 adsorption at 273 K for the characterization of porous carbons. Carbon. 2004; 42(7):1233–1242.
29. Nowakowski DJ, Jones JM, Brydson RMD, Ross AB. Potassium catalysis in the pyrolysis behaviour of short rotation willow coppice. Fuel. 2007; 86(15):2389–2402.
30. Pan WP, Richards GN. Influence of metal-ions on volatile products of pyrolysis of wood. J Anal Appl Pyrol. 1989; 16(2):117–126.
31. Raveendran K, Ganesh A, Khilar KC. Influence of mineral matter on biomass pyrolysis characteristics. Fuel. 1995; 74(12):1812–1822.
32. Wang ZY, Wang F, Cao JQ, Wang J. Pyrolysis of pine wood in a slowly heating fixed-bed reactor: Potassium carbonate versus calcium hydroxide as a catalyst. Fuel Process Technol. 2010; 91(8): 942–950.
33. Dimiev AM, Alemany LB, Tour JM. Graphene oxide. Origin of acidity, its instability in water, and a new dynamic structural model. Acs Nano. 2013; 7(1):576–588. [PubMed: 23215236]
34. Fan XB, Peng WC, Li Y, Li XY, Wang SL, Zhang GL, et al. Deoxygenation of exfoliated graphite oxide under alkaline conditions: A green route to graphene preparation. Adv Mater. 2008; 20(23): 4490–4493.
35. Wang H, Tian HW, Wang XW, Qiao L, Wang SM, Wang XL, et al. Electrical conductivity of alkaline-reduced graphene oxide. Chem Res Chinese U. 2011; 27(5):857–861.

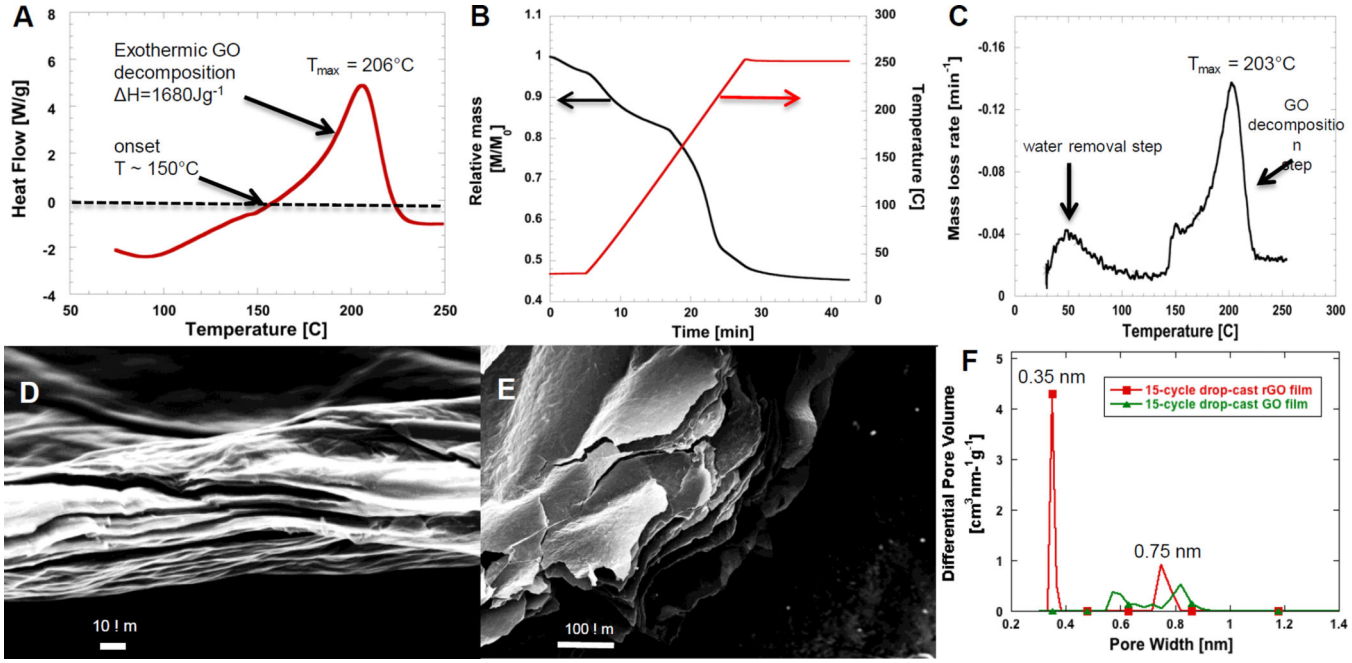

Figure 1.

Thermal analysis of the GO reduction process and pore structure of the rGO product. 1a) DSC thermogram of 15-cycle drop-cast GO film (1.1×10^5 GO layers) in 50 $mlmin^{-1}$ N_2 flow; heating rate 10 $Kmin^{-1}$, 1b) TGA thermogram of same GO film in 100 $mlmin^{-1}$ N_2 flow; heating rate 10 $Kmin^{-1}$, 1c) Differential TGA themgram of the same film, 1d) and 1e) SEM images of 9-cycle drop-cast GO film (6×10^4 GO layers) and 15-cyle drop-cast GO film (1.1×10^5 GO layers). These GO drop-cast films are reduced in the DSC under N_2 flow, heating rate 10 $Kmin^{-1}$ Fig. 1f) 15-cycle drop-cast GO and rGO film CO_2 isotherm NLDFT pore size distribution applying slit pore model.

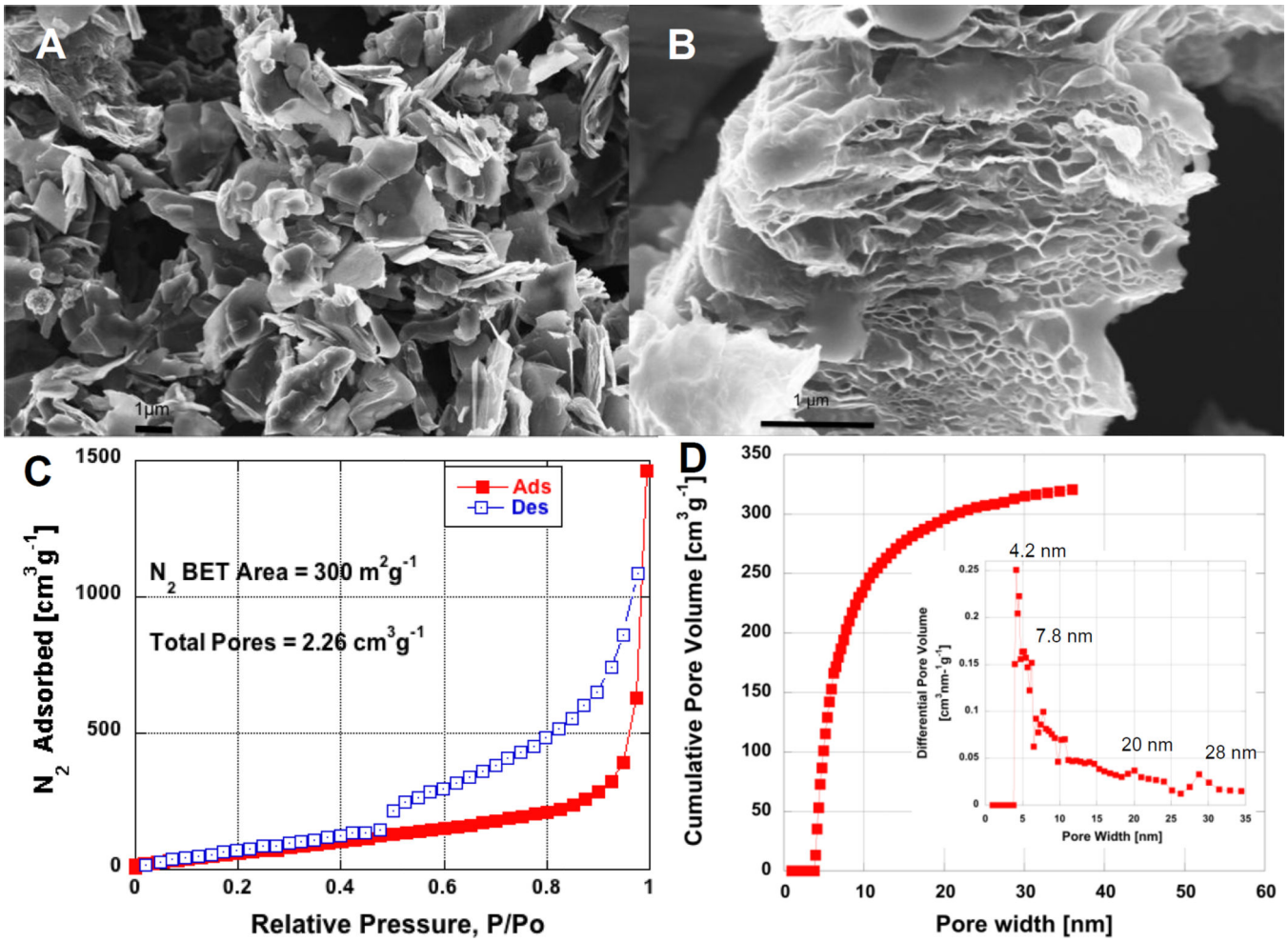

Figure 2.

Morphology and pore structure of powder produced by explosive thermal reduction of GO cake. 2a) and 2b) SEM images, 2c) N_2 vapor adsorption isotherm, 2d) N_2 isotherm NLDFT slit pore distribution.

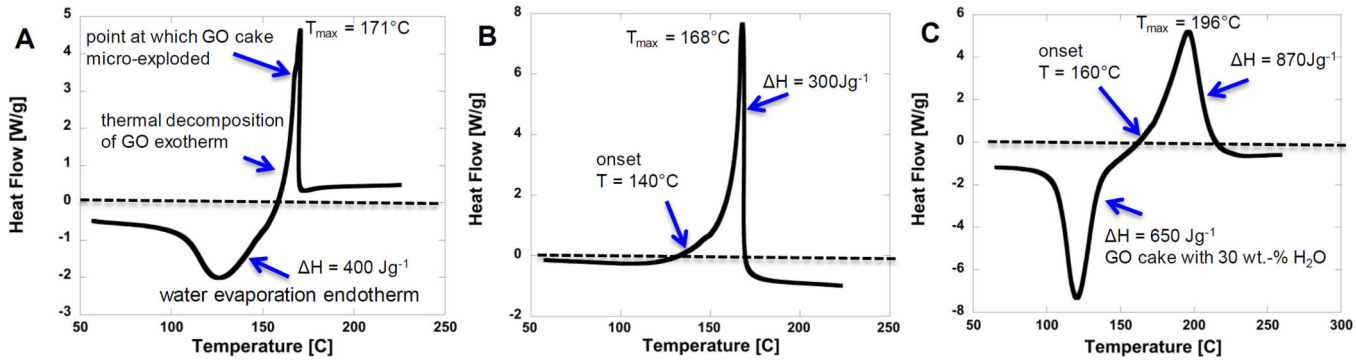

Figure 3.

Effect of interstitial water on the mode of GO thermal reduction (explosive vs. non-explosive). DSC thermograms 3a) GO cake which exploded during thermal reduction in N_2 gas, 3b) 24 hour low temperature oven dried GO cake (note GO cake still explodes after drying as indicated by the truncated asymmetric exotherm, 3c) humidified GO cake DSC thermogram (note large water endotherm and smooth exotherm indicating no explosion). Interstitial water does not cause or promote the explosive mode of GO reduction.

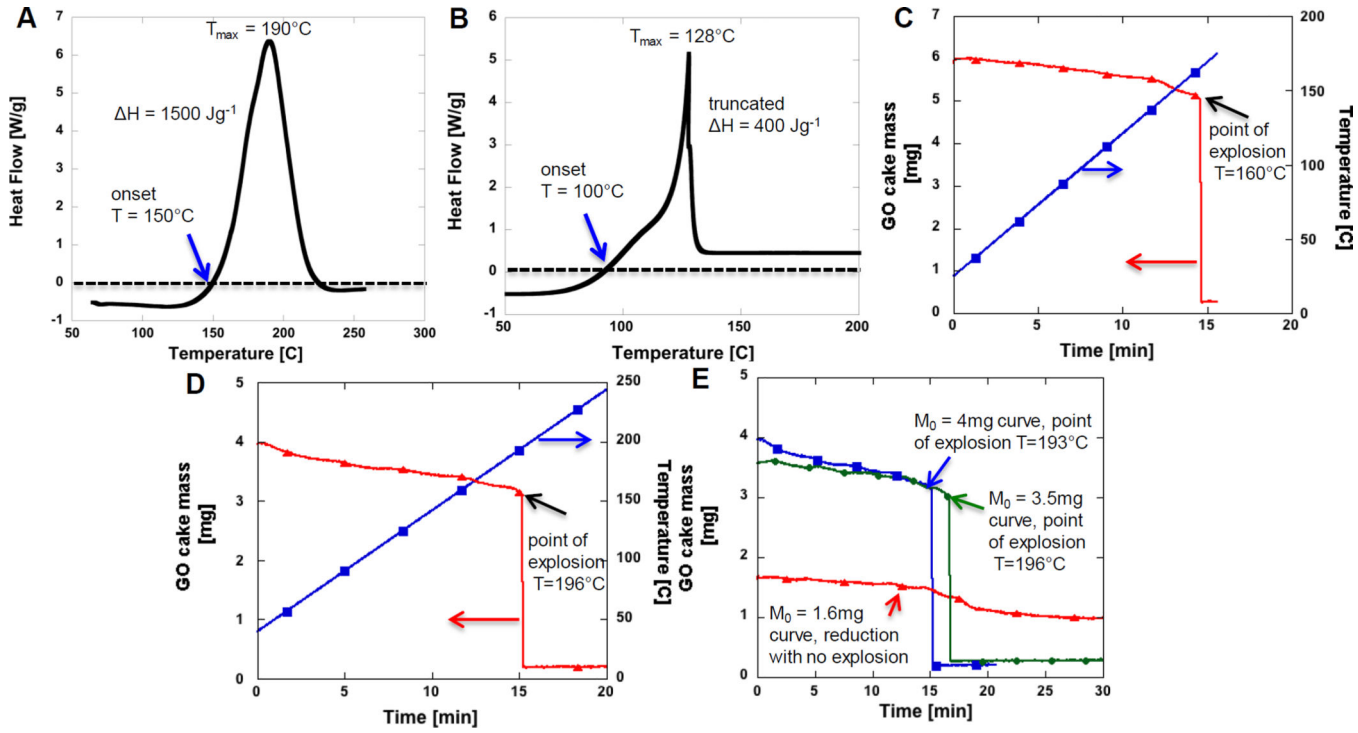

Figure 4.

Role of potassium hydroxide immersion, residual potassium content (K), and total sample mass in the explosive mode of GO reduction. 4a) DSC thermogram of GO cake that did not explode, 4b) DSC thermogram of the same cake immersed in 1 wt-% KOH solution and drying. Notice sharp exotherm indicating explosive reduction. 4c) and 4d) TGA thermograms of two different GO cakes 4c) GO cake which has 33 fold higher K content than the GO cake thermogram shown in 4d). Note the K effect to explosion temperature, sample with K (Fig. 4c) explodes at 36°C lower temperature compared to sample in Fig. 4d). Fig 4e) shows TGA thermogram of low K content GO cake varying initial sample mass in thermal reduction: 4mg, 3.5mg and 1.6 mg. Sample with 1.6 mg does not explode, while the larger GO masses do.

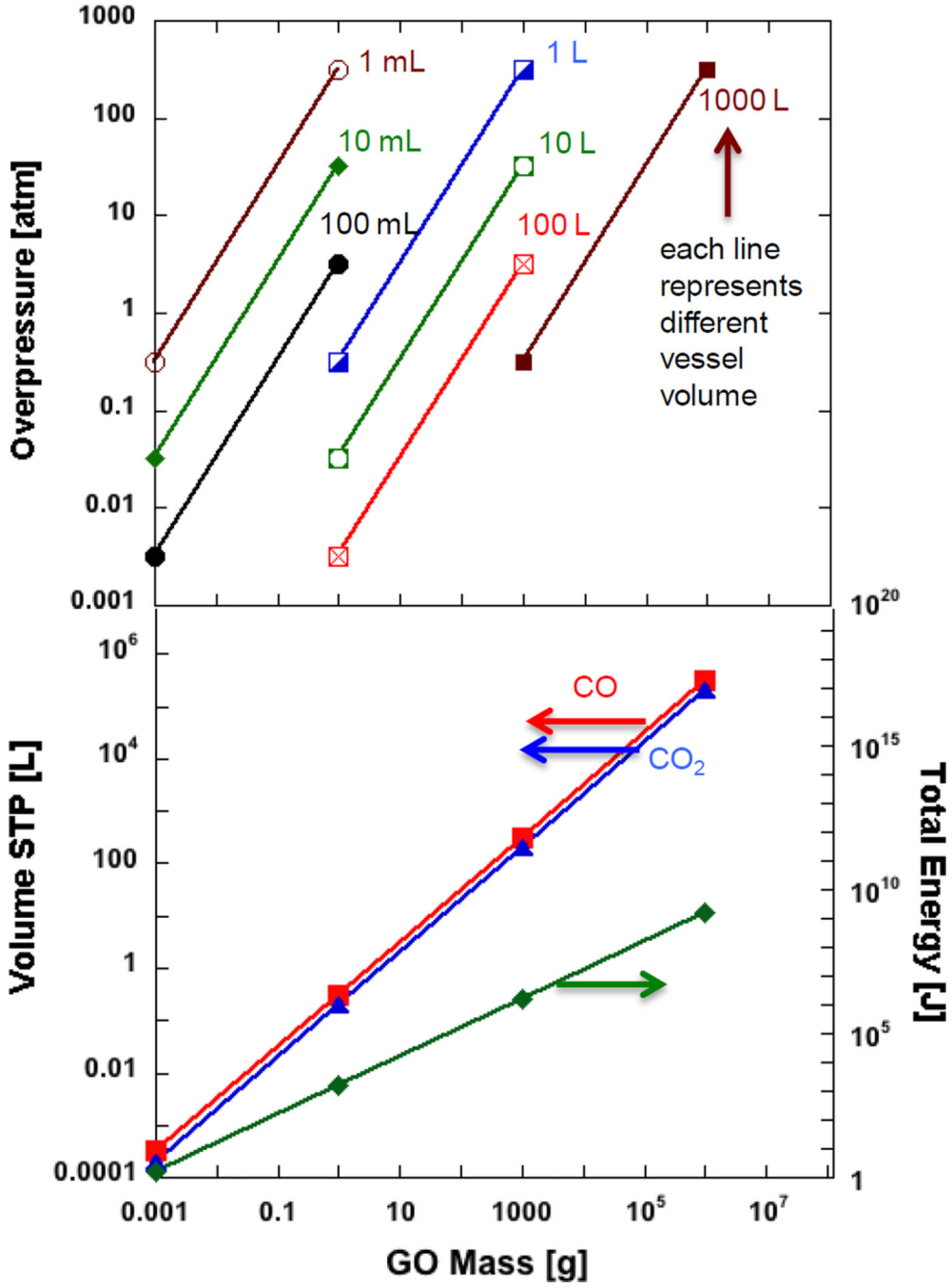

Figure 5.

Safety implications of GO explosive reduction. Bottom: total heat release and total evolved gas volume as a function of GO processing mass. The gas volume calculation was done for two limiting cases for the gas composition (pure CO_2 and pure CO), but the gas composition does not significantly affect the total volume estimates. Top: Estimated overpressure following unanticipated GO decomposition in sealed processing or storage vessels of various sizes.

Table 1

Measured thermochemical parameters of graphene oxide reduction.

GO film drop-cast cycle number	GO layer number (estimated from GO mass, Eq. 1)	Heating Rate, 10 $Kmin^{-1}$				Heating Rate, 50 $Kmin^{-1}$			
		GO Mass [mg]	T_{max} °C	Exothermic heat [Jg^{-1}]	Total Heat [J]	GO Mass [mg]	T_{max} °C	Exothermic heat [Jg^{-1}]	Total Heat [J]
6	3E+4	0.334	202	1568	0.524	0.463	230	1394	0.645
9	6E+4	0.648	200	1659	1.075	0.684	228	1459	0.998
12	9E+4	1.046	202	1639	1.714	1.064	227	1509	1.606
15	1.1E+5	1.242	206	1680	2.087	1.306	227	1457	1.903
GO cake	2.9E+5	3.250	190	1463	4.755	ND			

Carbon N Y. Author manuscript; available in PMC 2014 July 09.

Table 2

Decomposition enthalpies for graphene oxide and a selection of energetic materials and reactive industrial chemicals known to pose processing safety hazards associated with thermal runaway reactions.

Material/Chemical	Chemical application	Decomposition enthalpy, [Jg^{-1}]	Reference
Graphene oxide (GO)	Precursor for reduced GO	1400–1700	Current study
Benzoyl peroxide	Industrial chemical	1602	Severini et al. [22]
Cumene hydroperoxide	Industrial chemical	1219	Di Somma et al. [21]
Ethyl oleate ozonide	Industrial chemical	684	Cataldo F. [20]
Trinitrotoluene (TNT)	Monopropellant and explosive	2305	Ksiazczak A. [18]
Hydrazine	Monopropellant and explosive	2980–4906	Jang et al. [17]
Nitrocellulose	Monopropellant and explosive	1900–2400	Sovizi et al. [19]